Supporting Information

Three-Dimensional Integration of Black Phosphorus Photodetector with Silicon Photonics and Nanoplasmonics

Che Chen, Nathan Youngblood, Ruoming Peng, Daehan Yoo, Daniel A. Mohr, Timothy W. Johnson, Sang-Hyun Oh and Mo Li[*]

Department of Electrical and Computer Engineering, University of Minnesota, Minneapolis, Minnesota, 55455, USA.
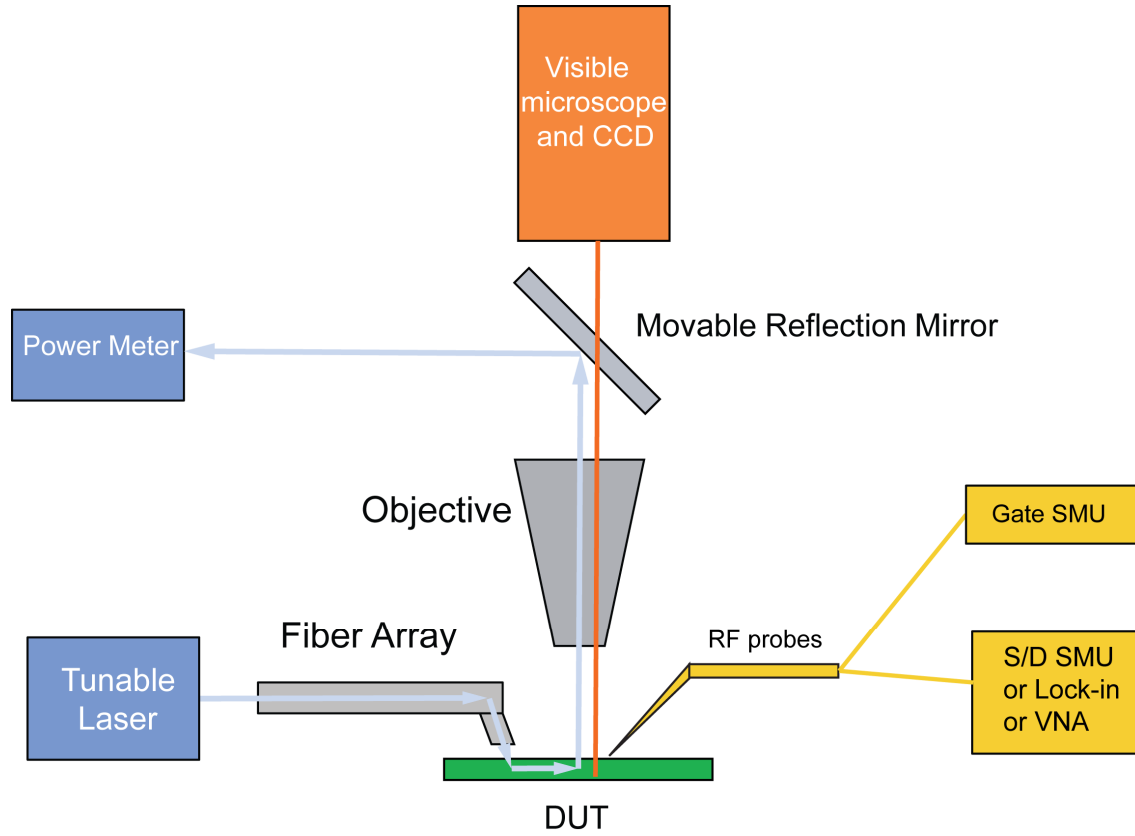
1. Measurement setup

Fig. S1. Measurement setup. Measurement setup used in the experiment. Not all components and connections are shown in the illustration.

In order to measure optical and electrical performance of the device, we use a measurement setup as shown in Fig. S1. To characterize emission efficiency of the silicon waveguide grating, telecom laser light is coupled into the waveguide via a customized fiber array and on-chip grating coupler. The light is guided to the waveguide grating and emitted vertically into free space which is collected by an infrared objective lens. When the removable reflection mirror (1550 nm band) is presented, the collected light is reflected to an optical power meter. Without the presence of the movable mirror, a visible microscope and CCD are used to locate device position. In the electrical measurement, the device has three contacts (source, drain and gate) which are connected to measuring equipment through high speed RF probes. A gate SMU is used to control the gate bias voltage during the entire measurement. For DC measurements, another SMU is connected to S/D contacts to measure current. In low frequency RF measurements, a low-noise amplifier (Stanford Research Systems SR570) amplifies the photocurrent, and a lock-in amplifier (Stanford Research Systems SR830) is used to measure electrical signal. In high RF frequency measurements, a VNA (Agilent 4396B) is used to measure the photoresponse for frequencies greater than 100 kHz. During RF frequency

measurements, the laser light is modulated by an electro-optical modulator (EOM, Lucent 2623NA) which is driven by a signal generator or the VNA output.
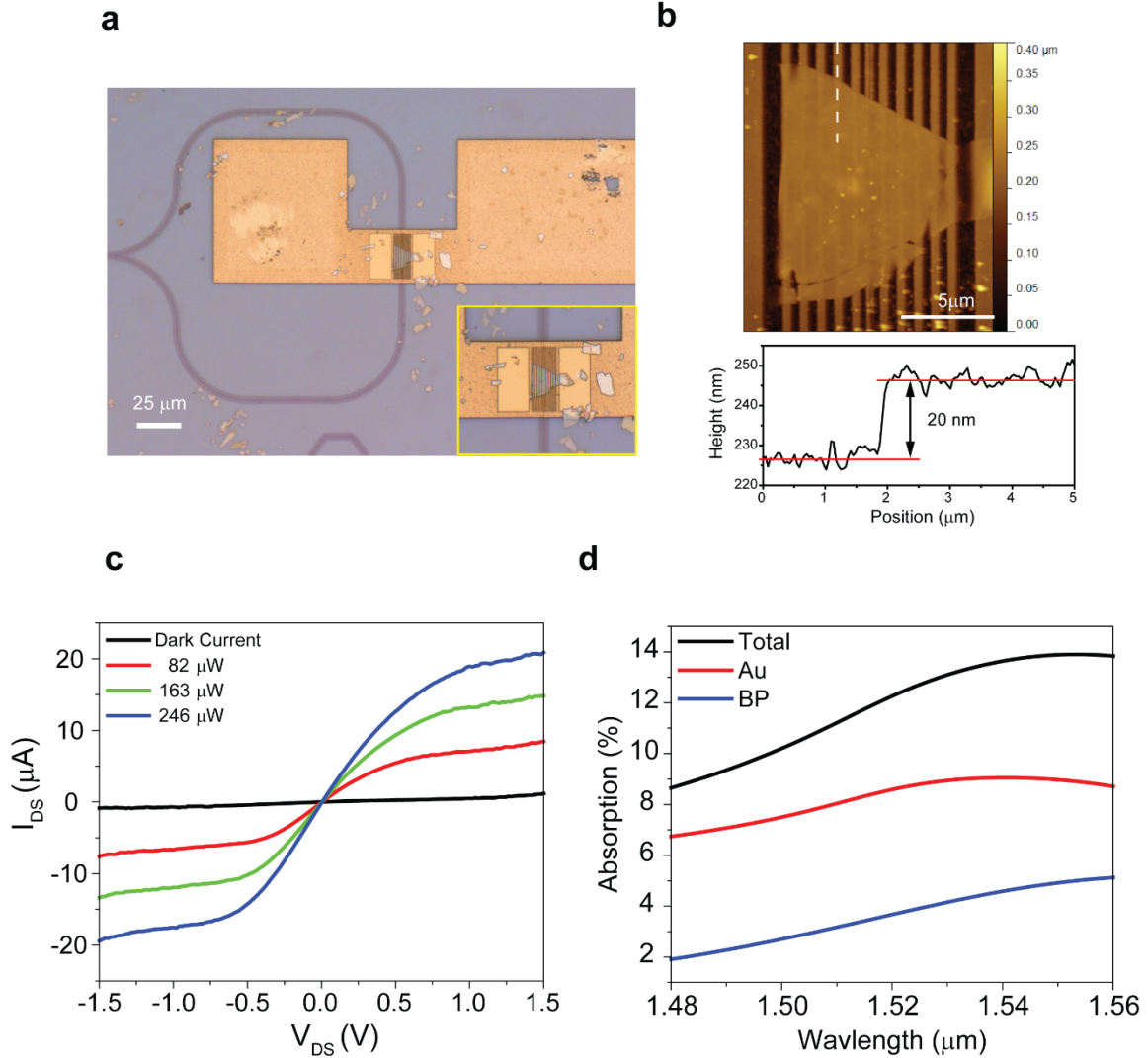
2. Second device without top gate

a

b

c

d

Fig. S2. BP photodetector without gate. (**a**) Microscope image of the fabricated device. Inset: zoom-in image of BP on nanogap. (**b**) AFM image of the BP flake on metallic grating. Lower panel: height profile of the flake along white dashed line indicating 20 nm thickness of BP. (**c**) I_{DS}-V_{DS} curves under different input optical powers. The marked optical power levels refer to the emission power at the waveguide grating, determined by our measurement. (**d**) Simulated absorption of Au and BP in the device without top metal gate. The absorption is normalized to optical emission of waveguide grating.

Here we show another fabricated device without a top metal gate. The intrinsic responsivity of this ungated device is shown in Fig. 4 (e) in main text. As shown in Fig. S2 (a), the overall structure is the same as the gated device in main text. AFM image (Fig. S2 (b)) indicates the BP flake has a length of 10 um and thickness of 20 nm. I_{DS}-V_{DS} measurements are shown in Fig. S2 (c) with various optical powers. Without optical illumination, the device has very small dark current. When input optical power increases, S/D current increases indicating the presence of photocurrent. I_{DS} is symmetric for positive and negative V_{DS}, which is different from the device in main text (Fig. 4 (a)). Fig. S2 (d) is the simulated absorption in different materials for this device (normalized to waveguide grating emission). Comparing to the 11% absorption in BP (Fig. 1 (e)) for a device with gate reflection, the absorption here is only 5% due to the absence of reflection from metal gate.
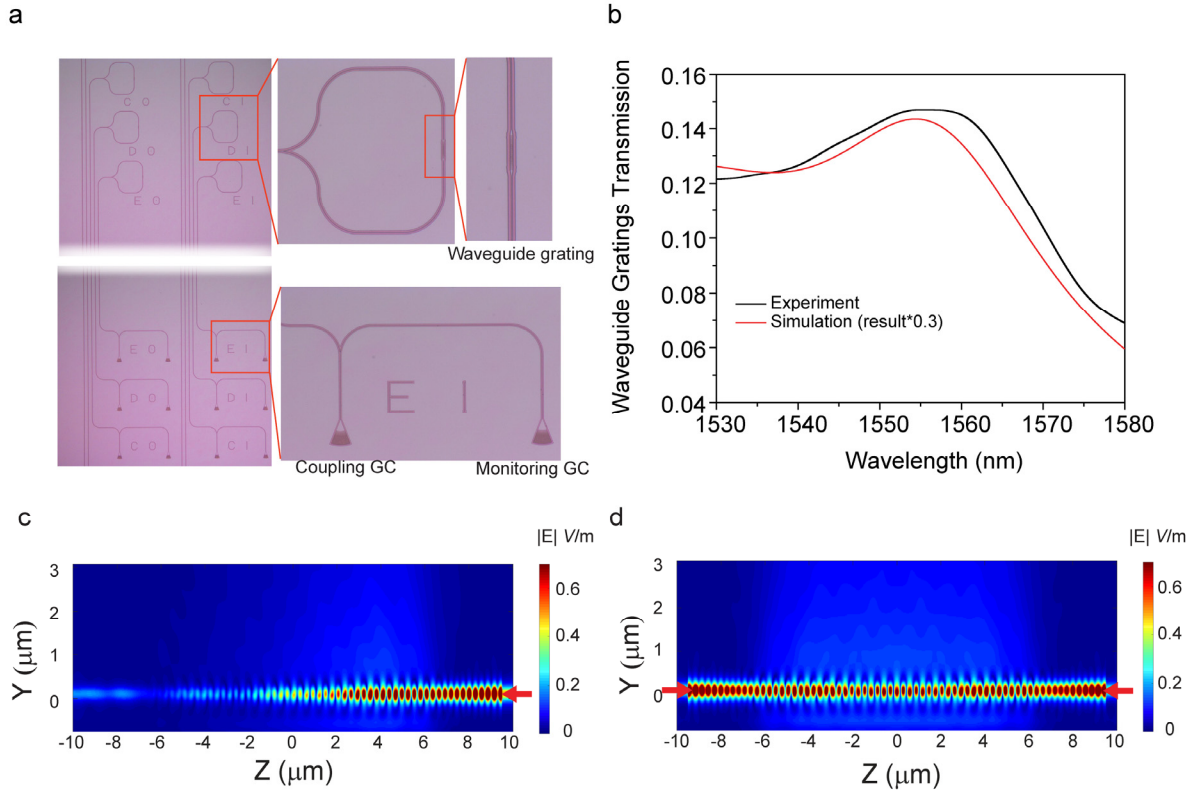
3. Silicon photonic layer design

Fig. S3. Photonic layer design and measurement. (**a**) Microscopic images of photonic layers. Two grating couplers (GC) are shown in right lower panel. Racetrack waveguide and waveguide grating are shown in the upper panel. (**b**) Measured waveguide grating transmission and simulated result. The transmission is normalized to the optical power in waveguide. (**c**) (**d**) Simulated (FDTD) E-field amplitude |E| for the waveguide grating cross-section (along light propagation direction) for (**c**) light input from right end only and (**d**) light input from both ends (indicated by red arrows).

The silicon photonic layer has two grating couplers (GC) as shown in Fig. S3 (a). The left GC is used to couple laser light into waveguide and the right one is used to monitor coupling efficiency after the first Y-split. The second Y-split divides light into two waveguides which recombine in the waveguide grating. The measured waveguide gating transmission spectrum (normalized to optical power in waveguide) is shown in Fig. S3 (b) with simulation result. The experiment and simulation spectra have similar shapes. However, measured waveguide grating efficiency is about 30% of the simulation result. This may be due to imperfections in fabrication.

Fig. S3 (c) (d) shows the simulated (FDTD) electric field amplitude distributions of the waveguide grating cross-section view. In Fig. S3 (c), only one source is injecting light from right side while in Fig. S3 (d), two light sources are placed on both sides of the grating and injecting light simultaneously. Apparently from the field distribution, the second scenario results in a better uniformity of the output wave front comparing to only one light source. This is more desirable for our application to couple light into plasmonic structure on top of silicon waveguide grating. So in our design, the light is split into two waveguides through the second Y-junction before emitted by waveguide grating.
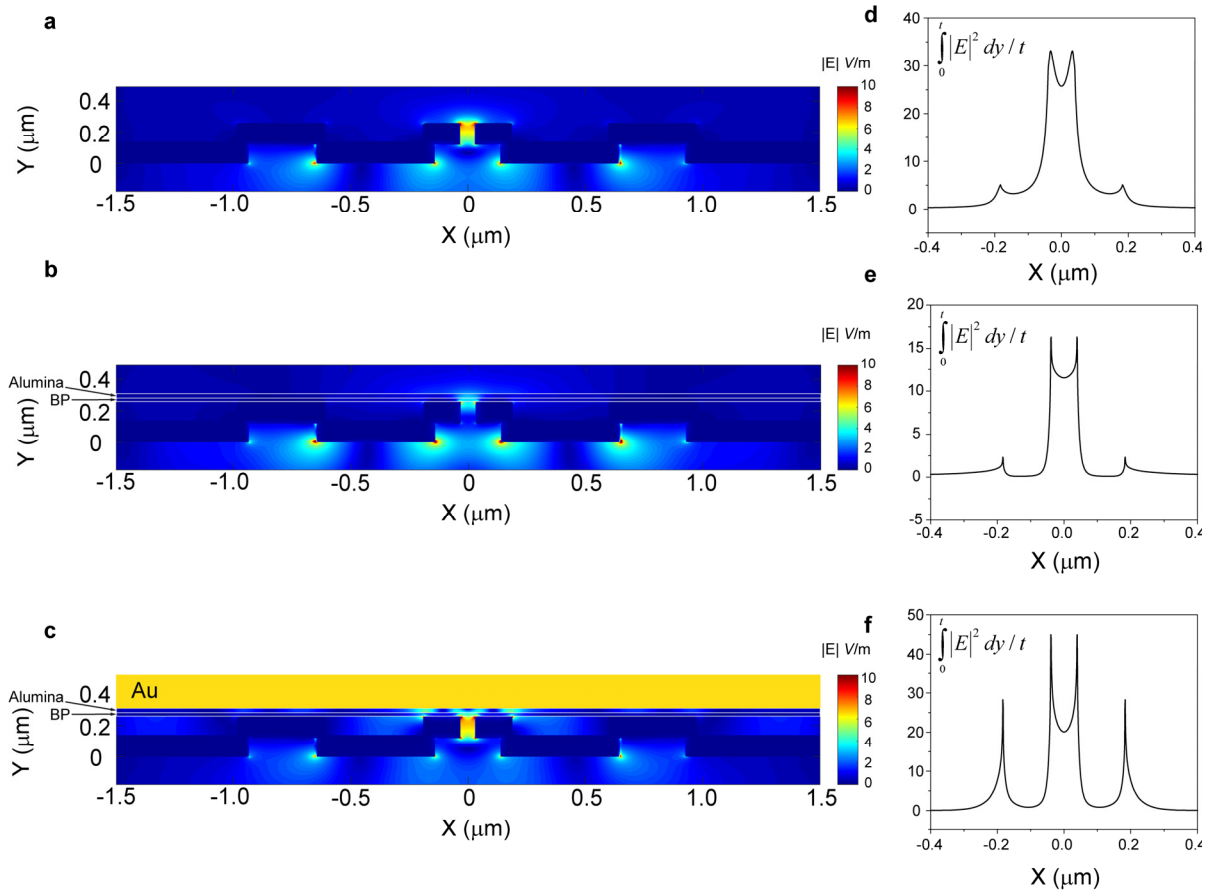
4. FDTD simulation

Fig. S4. FDTD simulation of plasmonic effect in devices including different layers. Electric field amplitude |E| distribution (left side) and average optical intensities within 20 nm above plasmonic gratings (right side) of devices including different layers: (**a**) (**d**) only metallic plasmonic gratings, (**b**) (**e**) BP and alumina are on top of metallic gratings, (**c**) (**f**) completed device with BP, alumina and top metal gate.

In order to verify plasmonic enhancement and gate metal reflection, a 2D FDTD simulation is performed for the device including different layers. Given the very large aspect ratio of the nanogap, 60 nm width and 25 μm length, 2D simulation provides sufficient precision and 3D simulation is rather unnecessary. Fig. S4 (a) shows the electric field distribution in metallic gratings. Fig. S4 (d) is the averaged optical intensity 20 nm above the top of plasmonic gratings. Fig. S4 (b) shows the electric field amplitude when BP and alumina layers are presented in the device. Fig. S4 (e) is the average optical intensity inside BP layer (20 nm). This corresponds to the ungated device shown in supplementary material. In Fig. S4 (c), the electric field distribution of the complete device including top metal gate is shown. The average optical intensity in BP layer (20 nm) is shown in Fig. S4 (f). Comparing Fig. S4 (e) and Fig. S4 (f), it is obvious that by adding a metal gate, optical intensity inside BP layer is enhanced which should increase optical absorption subsequently.

5. Plasmonic grating design
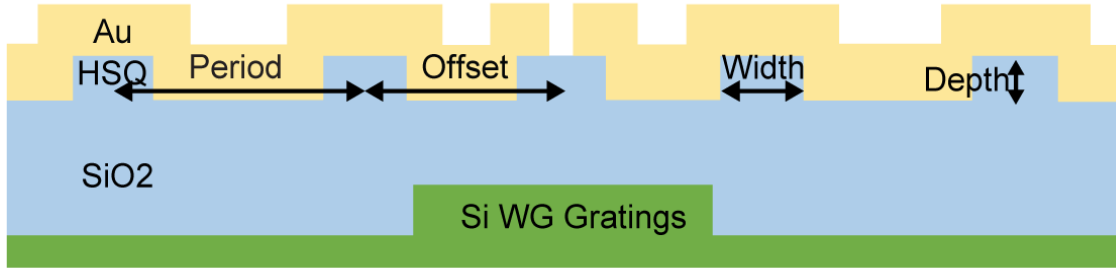
Fig. S5. Plasmonic grating cross section view and key design parameters.